

 Open access • Journal Article • DOI:10.1364/OL.15.000556

Iterative generation of holograms on spatial light modulators — [Source link](#)

[Uri Mahlab](#), [Joseph Rosen](#), [Joseph Shamir](#)

Institutions: [Technion – Israel Institute of Technology](#)

Published on: 15 May 1990 - [Optics Letters](#) (Optical Society of America)

Topics: [Spatial filter](#), [Iterative learning control](#) and [Holography](#)

Related papers:

- [Simulation, registration, and reconstruction of digital holograms of arbitrary objects by means of liquid crystal on silicon spatial light modulator](#)
- [Electro-optic hologram generation on spatial light modulators](#)
- [Iterative Fourier Transform Algorithm Based on the Segmentation of Target Image for a High-Speed Binary Spatial Light Modulator](#)
- [Optical implementation of iterative Fourier transform algorithm using spatial light modulator](#)
- [Extremely simple holographic projection of color images](#)

Share this paper:    

View more about this paper here: <https://typeset.io/papers/iterative-generation-of-holograms-on-spatial-light-4wsfo0kgma>

Iterative generation of holograms on spatial light modulators

Uri Mahlab, Joseph Rosen, and Joseph Shamir

Department of Electrical Engineering, Technion-Israel Institute of Technology, Haifa 32000, Israel

Received November 29, 1989; accepted March 12, 1990

Iterative learning procedures on a hybrid electro-optic system can be employed to generate holograms on inexpensive liquid-crystal-television spatial light modulators. The algorithm takes into account random electronic noise in the system and compensates for spatial-light-modulator distortions. Experimental results are given for the reconstruction of intensity distribution, and computer simulations demonstrate the possibility of a complete complex amplitude reconstruction.

Most of the recently considered architectures for optical signal processing contain computer-generated holograms or spatial filters. It is frequently desired to update these components in real time by employing spatial light modulators (SLM's). Unfortunately, when computer-generated components are displayed on currently available SLM's, their performance is substantially deteriorated owing to limited information capacity, distortions, and interpixel dead regions. The objective of this research is the implementation of iterative processes directly on a hybrid electro-optic system with no intermediary photographic or lithographic steps. A binary hologram is to be generated on a given SLM in such a way that it reconstructs a desired wave front when illuminated with coherent light. As an example, we demonstrate the procedure for a Fourier-transform hologram that uses the experimental system shown in Fig. 1. The transmittance of the SLM may be represented by a vector \mathbf{H} with elements $H_{kl} \in \{0, 1\}$. The lens performs an optical Fourier transform, \mathcal{F} , which yields the two-dimensional vector, $\mathbf{h} = \mathcal{F}\mathbf{H}$, with elements h_{kl} . The squared absolute values of these vector elements (not binary), $I_{kl} = |h_{kl}|^2$, are observed by the charge-coupled-device (CCD) camera.

Storing a reference pattern \mathbf{f} , we intend to generate a vector \mathbf{H} that will reconstruct, under coherent illumination, an output intensity distribution I_{kl} close to $|f_{kl}|^2$ within a given region of the output plane. The difference between I_{kl} and $|f_{kl}|^2$ can be characterized by an error function that should be minimized by successive iterations. With the method of Refs. 1 and 2, the error function is the mean-square error that, for the n th iteration, is defined by the relation

$$e_n = \frac{1}{N^2} \sum_{k,l=1}^N [|f_{kl}|^2 - \gamma_n I_{kl}^{(n)}]^2, \quad (1)$$

where the inspected region of the output plane contains N^2 pixels and γ_n is a parameter that compensates for the difference between the reconstructed intensity and the stored reference pattern,

$$\gamma_n = \frac{\sum I_{ij}^{(n)} |f_{ij}|^2}{\sum [I_{ij}^{(n)}]^2}. \quad (2)$$

In the next iteration, a small perturbation is induced on the vector \mathbf{H} to yield a new value for the error function, e_{n+1} . This iteration is accepted or rejected following criteria to be discussed below. Successful learning algorithms¹⁻³ in computer simulations failed when employed for the system of Fig. 1 owing to system noise, in particular that within the CCD camera and the SLM. To demonstrate the effect of this random noise, several measurements of the error function [Eq. (1)] were made for the same vector \mathbf{H} , with the results given in Fig. 2. All conventional optimization procedures investigated with this system (direct binary search, simulated annealing, etc.) were sidetracked by the random noise and never converged.

The breakdown of the iterative procedure occurs when, owing to a random noise fluctuation, the calculated error jumps to an unreasonably small value that cannot be approached by subsequent iterations. To avoid such a locking into an unphysical value of the error function, one should modify the acceptance criterion by assuming that a small perturbation on the input pattern cannot yield a large change in the error function. To estimate the acceptance limitations, we first calculate, for each iteration, the standard deviation of e_n until that iteration,

$$\sigma_n = \left[\frac{1}{n} \sum_{j=1}^n \left(e_j - \frac{1}{n} \sum_{i=1}^n e_i \right)^2 \right]^{1/2}. \quad (3)$$

Defining the change of the error function by

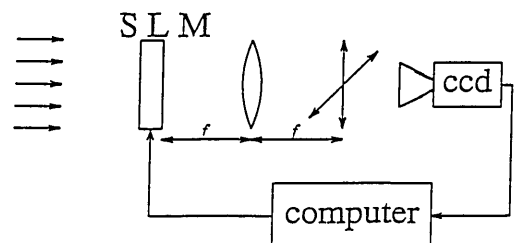


Fig. 1. Experimental system. The pattern generated on the SLM is Fourier transformed by the lens and observed by the CCD camera.

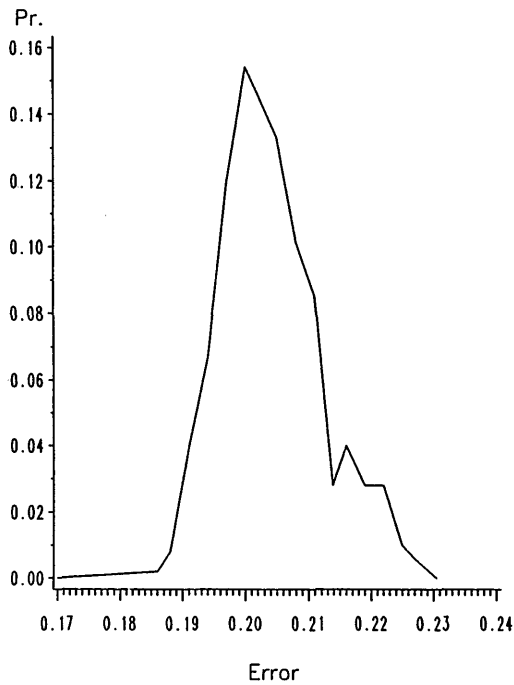


Fig. 2. Probability (Pr.) distribution of the error function for different measurements on the same hologram.

$$\Delta e_{n+1} = e_{n+1} - e_n, \quad (4)$$

we shall consider iterations for acceptance only if

$$|\Delta e_{n+1}| < \sigma_n. \quad (5)$$

Within this region, an iteration yielding a negative value,

$$\Delta e_{n+1} < 0, \quad (6)$$

will be accepted. With a simulated annealing type of algorithm, a positive value may be also accepted conditionally.

As an example we used a direct binary search^{1,2} to generate a hologram \mathbf{H} such that the intensity distribution of its Fourier transform corresponds to the letter \mathbf{F} , which is stored in the computer as a reference pattern. The image sequence of Fig. 3 shows the reconstruction from a binary hologram of 64×64 pixels presented on an array of similar size. Each image in the sequence represents one search cycle, which consists of 64×64 single-pixel updates.

Generation of holograms by the above procedure leads to the construction of a wave front with a predetermined intensity distribution over a given plane. We show now that, to control the phase distribution also, it is adequate to add the measurement of the value at the origin of the cross correlation between the reference and the hologram reconstruction. To do this we prove the following theorem:

Theorem: If

$$I_{kl} = |h_{kl}|^2 = |af_{kl}|^2, \quad k, l = 1, 2 \dots N, \quad (7)$$

with a a constant, and if

$$\left| \sum_{k,l=1}^N h_{kl}^* f_{kl} \right|^2 = \left| a \sum_{k,l=1}^N |f_{kl}|^2 \right|^2, \quad (8)$$

then

$$h_{kl} = af_{kl}. \quad (9)$$

Proof: According to the Schwartz inequality,

$$\left| \sum_{k,l=1}^N h_{kl}^* f_{kl} \right|^2 \leq \sum_{k,l=1}^N |h_{kl}|^2 \sum_{k,l=1}^N |f_{kl}|^2. \quad (10)$$

Substituting from condition (7), we have

$$\left| \sum_{k,l=1}^N h_{kl}^* f_{kl} \right|^2 \leq \left| a \sum_{k,l=1}^N |f_{kl}|^2 \right|^2. \quad (11)$$

Since the equality [condition (8)] holds when, and only when, relation (9) is satisfied, this proves the theorem. Furthermore, if \mathbf{h} is generated by minimizing the error function of Eq. (1), the limiting value of $|a|$ tends to $1/\sqrt{\gamma}$.

The left-hand side of condition (8) is the intensity at the origin of the cross correlation $C_{hf}(0)$ between \mathbf{h} and \mathbf{f} , while the right-hand side is the peak intensity of the autocorrelation function, $C_{ff}(0)$ of \mathbf{f} , which can be calculated and stored in a computer memory. The cross-correlation function can be measured and used for an optimization process⁴ by employing a system such as that shown in Fig. 4. The hologram is to be generated on the SLM. In our procedure, we display simultaneously on the input plane a point source and the reference function side by side. On the output plane, at the conjugate position for the delta function the point-spread function of the hologram will be displayed, while the cross-correlation function will be projected onto the region conjugate to the reference pattern on the input plane.



Fig. 3. Sequence of reconstructed patterns for consecutive iteration cycles. Each cycle is 64×64 single-pixel updates.

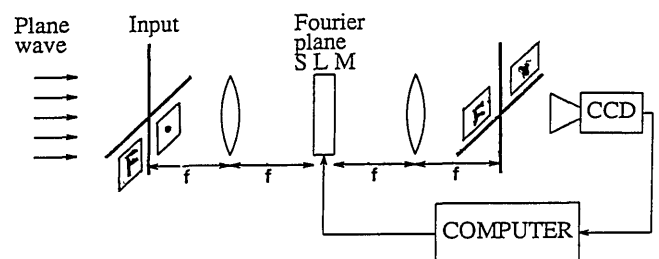


Fig. 4. System for complex amplitude reconstruction.

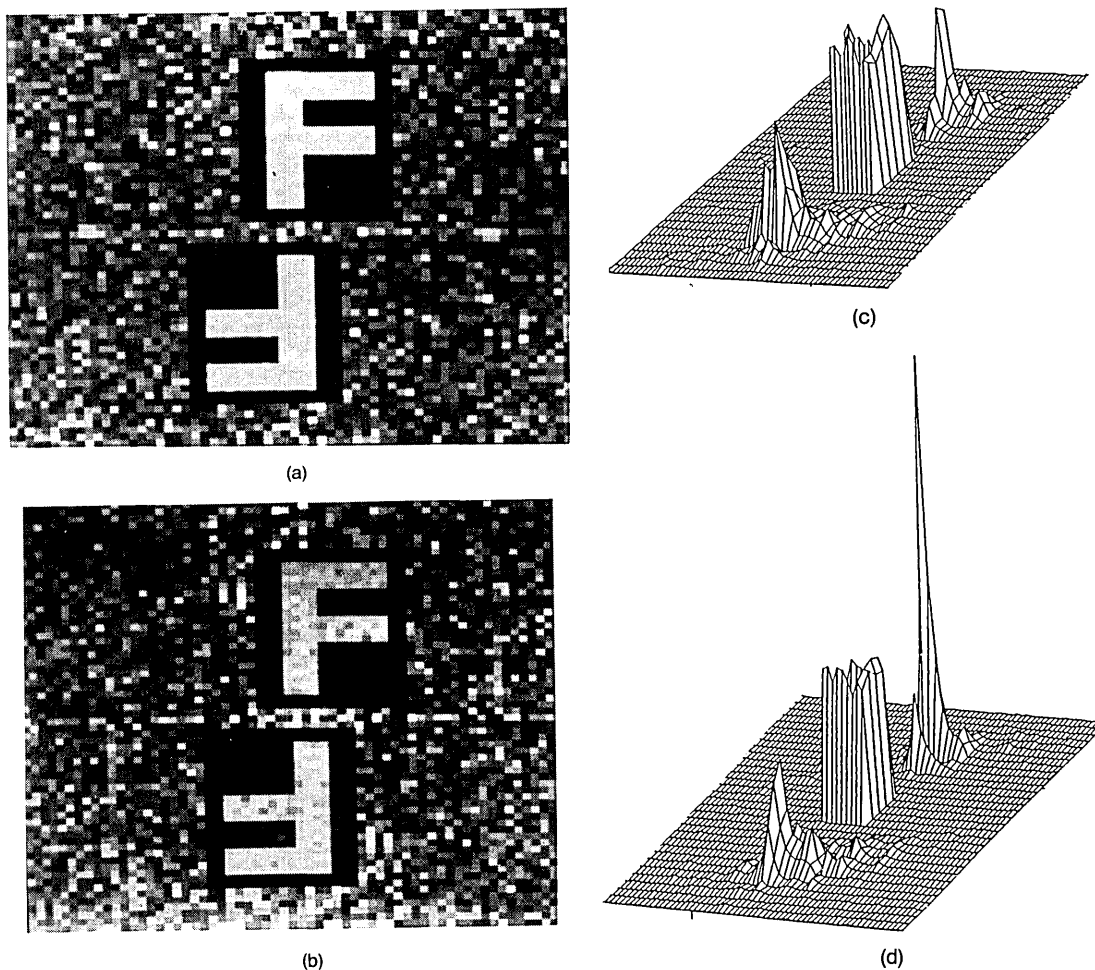


Fig. 5. Reconstructed object (with zero order suppressed) from (a) the hologram containing magnitude information only and from (b) the hologram conditioned by magnitude and phase information. (c) Cross-correlation function of the reference pattern with the point-spread function of hologram corresponding to (a), and (d) cross-correlation function of the reference pattern with the point-spread function of hologram corresponding to (b).

In addition to an error function similar to Eq. (1), we define now a second error function,

$$e_n^c = \| |C_{ff}(0)|^2 - \gamma_n |C_{hf}^{(n)}(0)|^2 \|. \quad (12)$$

This error function depends on a single number, $|C_{hf}(0)|^2$, which is relatively easy to measure. Thus, if the relation

$$\Delta e_{n+1}^c = e_{n+1}^c - e_n^c \leq 0 \quad (13)$$

is satisfied, conditions (5) and (6) will be considered for acceptance of the iteration. The results of a computer simulation are shown in Fig. 5. Figure 5(a) is the Fourier-transformed reconstruction of the hologram with the intensity constraint only, while for the generation of the hologram corresponding to Fig. 5(b) the magnitude *and* the phase were taken into account. In Figs. 5(c) and 5(d) the respective intensity distributions are given for the cross correlation of the reference pattern, the letter F, with the point-spread function of the two holograms. Although the intensity distribution of the point-spread function in Fig. 5(a) looks

better (it is easier to satisfy one condition than two), the high correlation peak of the second hologram demonstrates a much better reconstruction of the complex amplitude. In fact, the height of the correlation peak is 91% of the autocorrelation peak for the reference pattern, which indicates an excellent convergence toward the phase distribution of the reference pattern.

In conclusion, we have demonstrated direct generation of holograms on low-quality SLM's in the presence of system noise. The possibility of recording the complete complex amplitude information, magnitude, and phase was proved theoretically and by computer simulations.

References

1. M. A. Seldowitz, J. P. Allebach, and D. W. Sweeney, *Appl. Opt.* **26**, 2788 (1987).
2. B. K. Jennison, J. P. Allebach, and D. W. Sweeney, *Opt. Eng.* **28**, 629 (1989).
3. J. P. Allebach and D. W. Sweeney, *Proc. Soc. Photo-Opt. Instrum. Eng.* **884**, 2 (1988).
4. U. Mahlab and J. Shamir, *Opt. Lett.* **14**, 1168 (1989).